



Vlasov simulations of reconnection events and comparison with MMS

F. Califano¹, O. Pezzi², G. Cozzani^{1,3}, A. Retin³, F. Valentini², and G. Brunetti²

¹ Università di Pisa – Dipartimento di Fisica, Largo Bruno Pontecorvo 3, 56127 Pisa, Italy
e-mail: francesco.califano@unipi.it

² Università della Calabria – Dipartimento di Fisica, via Pietro Bucci, 87036 Arcavacata di Rende (CS), Italy

³ CNRS – LPP UMR 7648, Ecole Polytechnique, route de Saclay, 91128 Palaiseau Cedex, France

Abstract. The main goal of this project is to perform realistic fully-kinetic Vlasov simulations of magnetic reconnection aimed at reproducing the physics of reconnection sites at kinetic scales observed by MMS spacecraft measurements. To this end, we integrate the Vlasov equations for electrons and protons by adopting an Eulerian approach that ensure a low-noise description in particular at small scales. However, this approach is more time consuming and memory demanding than the standard Lagrangian PIC approach. For this reason, instead of coupling the Vlasov equation to the full Maxwell set of equations, we adopt the so-called Darwin approximation by which we solve the Maxwell equation but excluding light waves. This allows us to significantly increase the time step while maintaining all the main physics underlying the reconnection process. Specific goals are the evaluation of the generalized Ohm's law including anomalous resistivity terms and the study of wave-particle interactions around reconnection sites. Realistic initial conditions will be provided by MMS observations of reconnection at the Earth's magnetosphere. This project has to be considered as the starting point of a long time research project. We are presently starting a study period of code optimization to be in the condition for applying to a PRACE project.

1. Introduction

The magnetosphere–solar wind environment is an excellent natural plasma physics laboratory, in particular for what concerns the study of the process of magnetic reconnection. Very accurate high-resolution measurements are today available by in-situ spacecraft observations. Two main regions are the locations in near-Earth space where magnetic reconnection occurs, the magnetopause and the magnetotail current sheet. Magnetopause reconnection occurs between two different plas-

mas leading to the so-called non-symmetric reconnection, while magnetotail reconnection is symmetric. Reconnection is a very complex multi-scale process occurring locally in a very thin micro-layer but leading eventually to a large-scale rearrangement of the magnetic field topology together with a strong energy release. Observations have been performed for decades leading to a very good understanding of reconnection at large (fluid) scales, that is, scales much larger than the ion gyro-radius. These observations have been largely supported by a wealth of magneto-hydrodynamics (MHD)

simulations of symmetric reconnection, able to reproduce such a large-scale field reconfiguration of the system. A strong improvement has been achieved by multi-spacecraft measurements, as the one provided by the relatively recent Cluster mission, able to shed light on the critical internal layer at ion scale. Two-fluids and kinetic hybrid Particle-In-Cell simulations have supported such observations, in particular confirming the role of Hall physics at ion scales. On the other hand, the physics of reconnection at the smaller electron scales have been poorly understood until recently, when full PIC simulations have been able to reproduce the electron micro-layer embedded in the ion layer. The electron micro-layer plays a fundamental role being the location where the magnetic field can eventually detach from and diffuse into the plasma. The investigation of the physics at electron scales is fundamental in order to understand how reconnection can locally violate the ideal MHD frozen-in constraint and how electrons are energized at the reconnection site. However, until recently, no measurements at the electron scale were available even in the laboratory because of technical reasons. This is one of the reasons which yields to the launch of the four spacecraft NASA/MMS mission in 2015. MMS aims at investigating, for the first time, the physics of reconnection at the electron scale thus allowing the reconnection community to test the predictions of kinetic numerical simulations and understand the electron reconnection dynamics.

With this INAF project, we have started a long-time project, aimed at studying numerically the magnetic reconnection process in order to interpret satellite data from the MMS mission which are available in our research group. We make use of a new model, namely the Vlasov-Darwin model, based on the direct integration of the electron and proton Vlasov equations self-consistently coupled to the Maxwell equations recasted such as to remove light waves. This approach allows us to significantly reduce the CFL constraint on the time step. We intend to address the problem of electron-scale reconnection physics by investigating how the electric field that leads to the onset of reconnection. Addressing this prob-

lem requires the evaluation of the so-called Generalized Ohm's law using both simulations and observational data. It is worth noticing that it is the first time that experimentally it is possible to measure the reconnection electron dynamics and that only very low noise simulations, such as the Eulerian Vlasov approach here adopted, are able to shed light on this fundamental problem.

This INAF project represents the starting point for several long term objectives: *i*) to establish the relative importance of kinetic terms such as the electron pressure tensor and inertia, *ii*) to investigate the role of the wave-particle interaction terms (the so-called anomalous resistivity). We also intend to show which wave modes dominate at reconnection sites and what is their role for the energization of ions and electrons. All these processes contribute to the reconnection electric field production. We believe that the synergy between simulations and experimental data is crucial to achieve this goal. So far, there are only a very few examples of high-resolution electron-scale kinetic simulations of magnetic reconnection. The outcome of this project are expected to represent a first achievement in reconnection physics understanding and it will prove valuable for the planning and scheduling of future space missions. For our research group this project is a basic step, a springboard, for future high-resolution simulations for which we intend to make a PRACE proposal in the next future.

The first part of the project has been supported by a INAF B computational grant, which has been of strategic importance for code development and testing. Indeed, it allowed us to start very rapidly our phase of code set up, testing and optimization on Marconi KNL. It gave us the proper resources at the good time. A computational paper where the results of several physical tests and code performance have been collected, has been recently submitted to an international peer-reviewed journal Pezzi (2019). Possible developments of our research will potentially open the way for future PRACE call, due to the very-huge computational resources needed for a full Vlasov code.

2. The Darwin approximation

The Darwin approximation has been adopted to reduce the limitations on the time steps for numerical integration (see for instance Mangeney 2002; Schmitz 2006). Indeed, since Maxwell equations allow for the propagation of waves at light speed c , the time step δt of any explicit numerical scheme solving these equations would be limited by the Courant-Friedrichs-Lewy (CFL) condition, $\delta t \lesssim \delta x/c$ Peyret (1983). The Darwin approximation, ruling out the transverse light waves corresponding to the fastest waves in the system propagating at phase speed c , significantly relaxes the CFL condition. In the following we list the Vlasov-Darwin system of equations, previously presented in a INAF B n. HP10BEQM02 project report, for the sake of self-consistency. The system of equations, composed by the Vlasov equations self-consistently coupled to the Maxwell's equations, reads (in CGS units):

$$\frac{\partial f_a}{\partial t} + \mathbf{v} \cdot \frac{\partial f_a}{\partial \mathbf{x}} + \frac{Z_a}{\mu_a} (\mathbf{E} + \mathbf{v} \times \mathbf{B}) \cdot \frac{\partial f_a}{\partial \mathbf{v}} = 0 \quad (1)$$

$$\nabla \cdot \mathbf{B} = 0; \quad \nabla \cdot \mathbf{E}_L = \zeta^2 n;$$

$$\nabla \times \mathbf{E}_T = -\frac{\partial \mathbf{B}}{\partial t}; \quad \nabla \times \mathbf{B} = \bar{w}^2 \frac{\partial \mathbf{E}_L}{\partial t} + \bar{w}^2 \zeta^2 \mathbf{j}$$

These equations are normalized using a characteristic length \bar{L} , time \bar{t} , velocity $\bar{U} = \bar{L}/\bar{t}$, mass \bar{m} . Then, the electric and magnetic fields are normalized to $\bar{E} = \bar{m}\bar{U}/e\bar{t}$ and $\bar{B} = \bar{m}c/e\bar{t}$. Furthermore, the following non-dimensional parameters are defined as: $\mu_a = \bar{m}/m_a$, $\bar{w} = \bar{U}/c$, $\zeta = \bar{\omega}_p \bar{t}$ where $\bar{\omega}_p = \sqrt{4\pi\bar{n}e^2/\bar{m}}$. Finally, the number and current density defined as $n = \sum_a Z_a n_a = \sum_a Z_a \int f_a d\mathbf{v}$ and $\mathbf{j} = \sum_a \mathbf{j}_a = \sum_a Z_a \int f_a \mathbf{v} d\mathbf{v}$, are normalized to \bar{n} and $\bar{n}e\bar{U}$, respectively. The equations for the electromagnetic field can be further simplified to obtain a set of Helmholtz-like equations of state that do not contain explicit time derivatives (see (Pezzi 2019) for details):

$$\nabla^2 \phi = -\zeta^2 n; \quad \mathbf{E}_L = -\nabla \phi; \quad \nabla^2 \mathbf{B} = -\bar{w}^2 \zeta^2 \nabla \times \mathbf{j} \quad (2)$$

$$\nabla^2 \mathbf{B} = -\bar{w}^2 \zeta^2 \nabla \times \mathbf{j}; \quad \nabla \cdot \mathbf{B} = 0; \quad (3)$$

$$\nabla^2 \hat{\mathbf{E}}_T - \bar{w}^2 \zeta^2 \sum_a \frac{Z_a^2 n_{a,0}}{\mu_a} \hat{\mathbf{E}}_T = \bar{w}^2 \zeta^2 \times \left[-\nabla \cdot \sum_a Z_a \langle \mathbf{v}\mathbf{v} \rangle_a + \sum_a \frac{Z_a^2}{\mu_a} (n_a \mathbf{E}_L + \langle \mathbf{v} \rangle_a \times \mathbf{B}) \right] \quad (4)$$

$$\nabla^2 \Theta = \nabla \cdot \hat{\mathbf{E}}_T \quad \mathbf{E}_T = \hat{\mathbf{E}}_T - \nabla \Theta \quad (5)$$

Equations (2)-(5) together with the Vlasov equation (1) with $a = e, p$, are integrated by adopting the splitting scheme in the e.m. limit (Mangeney 2002). In particular, the electron and proton Vlasov equations are integrated in the phase space $D_s \times D_v = [L_x, L_y, L_z] \times [M_{v_x}^a, M_{v_y}^a, M_{v_z}^a]$, where $M_{vi}^a = [-v_{a,i}^{max}, v_{a,i}^{max}]$, $a = e, p$ and $i = x, y, z$. We use $N_x \times N_y \times N_z$ grid points in space and $(2N_{a,v_x} + 1) \times (2N_{a,v_y} + 1) \times (2N_{a,v_z} + 1)$ in velocity. We set $v_{a,i}^{max}$ as a relatively big multiple (at least 5) of the thermal speed $v_{th,a}$ to ensure mass conservation.

3. Magnetic reconnection at electron scale

We have performed a $2D-3V$ symmetric magnetic reconnection simulation. The initial condition of our simulation is the one adopted in the GEM challenge (Birn 2001), in order to allow for a direct comparison to previous studies (Birn 2001; Schmitz 2006). For this reason, we have chosen the *hybrid* normalization ($\bar{L} = d_p$, $\bar{t} = \Omega_{c,p}^{-1}$, $\bar{U} = v_{A,p}$, the Alfvén velocity, $\bar{m} = m_p$).

The equilibrium is set by adapting the Harris equilibrium (Harris 1962) to periodic boundary conditions in the spatial domain. In particular, the equilibrium component of the magnetic field $B_x(y)$ is characterized by the presence of two gradients (corresponding to two current sheets) varying as an hyperbolic tangent as defined in Harris (1962) and located at $y = L_y/2$ and $y = 0$ (and so at $y = L_y$) where L_y is the length of the spatial domain in the y direction. The first hyperbolic tangent is characterized by a scale length L_1 , corresponding to the current sheet thickness. The thickness L_2 of the second current sheet is taken sufficiently large compared to L_1 to slow down

the development of reconnection there with respect to the main current sheet. The electron and ion temperature are set uniform at the initial time and the density $n(y)$ is defined in order to satisfy pressure balance. Then, from Eq. (3) and considering $\partial_t \mathbf{E}_L = 0$ at the initial time, we get the initial equilibrium current density $\mathbf{j} = (0, 0, j_z(y))$. Moreover, quasi-neutrality is imposed at $t = 0$, $n_e(y) = n_p(y) = n(y)$.

As for the GEM challenge (Birn 2001), fluctuations are superposed to the initial magnetic field in order to obtain a single magnetic island at the center of the space domain at the initial time. In particular, $\delta \mathbf{B} = \nabla \delta \psi \times \hat{z}$ and

$$\delta \psi(x, y) = \psi_0 \cos(2\pi x/L_x) \cos(2\pi y/L_y) \quad (6)$$

where, as already stated, L_x and L_y are the lengths of the spatial domain in x and y direction respectively. According to GEM challenge, in scaled units, ψ_0 is set to 0.1. By using the relation $\delta \mathbf{B}(x, y) = \nabla \delta \psi(x, y) \times \hat{z}$ and Eq.(3), we derive the expression for the current density fluctuations $\delta \mathbf{j}(x, y)$ consistent with $\delta \psi(x, y)$. Finally, the initial electron and proton distribution functions are shifted Maxwellian distributions with drift velocities along the z direction and temperature T_e and T_p .

For this run, the phase space has been discretized with $N_x \times N_y = 512 \times 512$ gridpoints in the spatial domain, $N_{e,v_x} \times N_{e,v_y} \times N_{e,v_z} = 41 \times 41 \times 81$ gridpoints in the velocity domain for electrons and $N_{p,v_x} \times N_{p,v_y} \times N_{p,v_z} = 31 \times 31 \times 31$ gridpoints in the velocity domain for protons. We also set $v_e^{max} = 5 v_{th,e}$ and $v_p^{max} = 5 v_{th,p}$, where the normalized $v_{th,p}$ is set to 1. Other simulation parameters are $L_1 = 0.5 d_p$, $L_2 = 2.5 d_p$, $m_p/m_e = 25$, $n_\infty = 0.2$, $T_e/T_p = 0.2$, $L_x = L_y = 25.6 d_p$. Also, we set $B_0 = 1$ and $n_0 = 1$.

In Figure 1 we show the contour plots of the out of plane magnetic field B_z (a), of the electron current density in the z -direction $j_{e,z}$ (b), of the proton current density in the z -direction $j_{p,z}$ (c) and of the electron number density n_e (d) in the phase of ongoing reconnection. In each panel, the contour lines of the magnetic flux ψ are superposed. B_z exhibits the typical Hall quadrupolar pattern usually observed during symmetric magnetic reconnection. We note that the $j_{p,z}$ pattern closely fol-

lows the density pattern ($n_e \approx n_p$) so that $j_{p,z}$ is depleted at the X point while it reaches its maximum value within the magnetic island. On the other hand, $j_{e,z}$ is enhanced at the X point and the region of strong $j_{e,z}$ is elongated along x . Away from the X point, $j_{e,z}$ splits into two branches that identify the separatrices. Other results are presented in Ref. Pezzi (2019).

We are also currently performing $2D-3V$ simulations in which the magnetic reconnection instability is not imposed through some magnetic field variation already present at $t = 0$. Indeed, the initial magnetic field and current density perturbations are random fluctuation composed by sines and cosines superposed over a current sheet so that magnetic reconnection is let free to develop. This approach is less used that the GEM challenge approach because of computational and technical reasons, but it will allow us to study the onset of magnetic reconnection, a problem which is still poorly understood. In Figure 2 we show preliminary results of this new simulation. At the beginning (panel (a)) the current sheet is almost unperturbed and B_z presents only fluctuations while after some time reconnection develops as demonstrated by the presence of an X-point structure and an associated quadrupolar B_z .

For this run, we use the *electromagnetic* normalization, i.e. $\bar{L} = d_e$, $\bar{t} = \omega_{p,e}^{-1}$, $\bar{U} = c$, $\bar{m} = m_e$. The phase space has been discretized with $N_x \times N_y = 512 \times 384$ gridpoints in the spatial domain, $N_{e,v_x} \times N_{e,v_y} \times N_{e,v_z} = 41 \times 41 \times 41$ gridpoints in the velocity domain for electrons and $N_{p,v_x} \times N_{p,v_y} \times N_{p,v_z} = 41 \times 41 \times 41$ gridpoints in the velocity domain for protons. We also set $v_e^{max} = 6 v_{th,e}$ and $v_p^{max} = 8 v_{th,p}$, where the normalized $v_{th,e}$ is set to 0.03 and $T_e = T_p$. Other simulation parameters are $L_1 = 2.5 d_e$, $L_2 = 3.75 d_e$, $m_p/m_e = 25$, $n_\infty = 0.2$, $T_e/T_p = 1.0$, $L_x = 102.40 d_e = 20.48 d_p$ and $L_y = 76.80 d_e = 15.36 d_p$.

4. Conclusion

In the present report we have summarized some of our recent results achieved through a new Eulerian Vlasov-Darwin code, recently developed at Cineca by our research group .

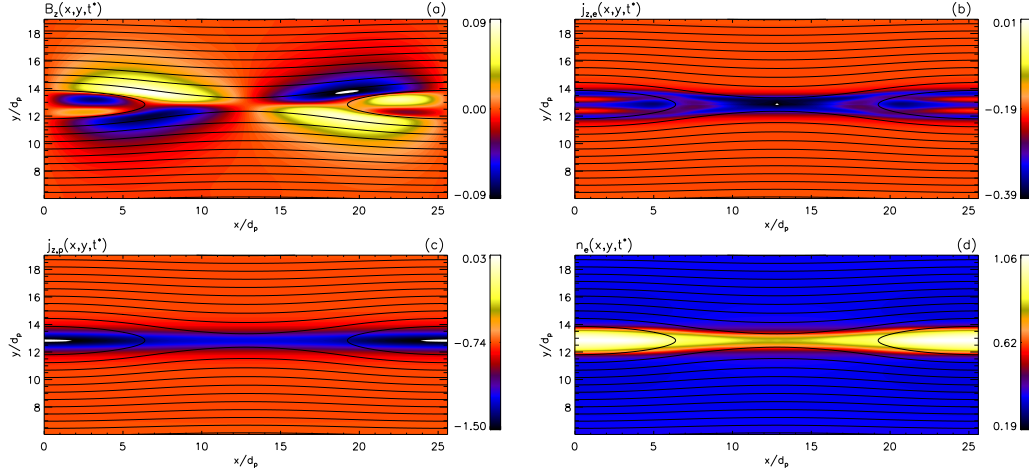


Fig. 1. Contour plots of B_z (a); out-of-plane electron current density $j_{e,z}$ (b); out-of-plane proton current density $j_{p,z}$ (c); and electron number density n_e (d). The quantities are shown at the time $t^* = 15.27 \Omega_{c,p}^{-1}$. At that time $\Delta\psi = 1.18$. All the panels are zoomed in y in the interval $[6 d_p, 19 d_p]$.

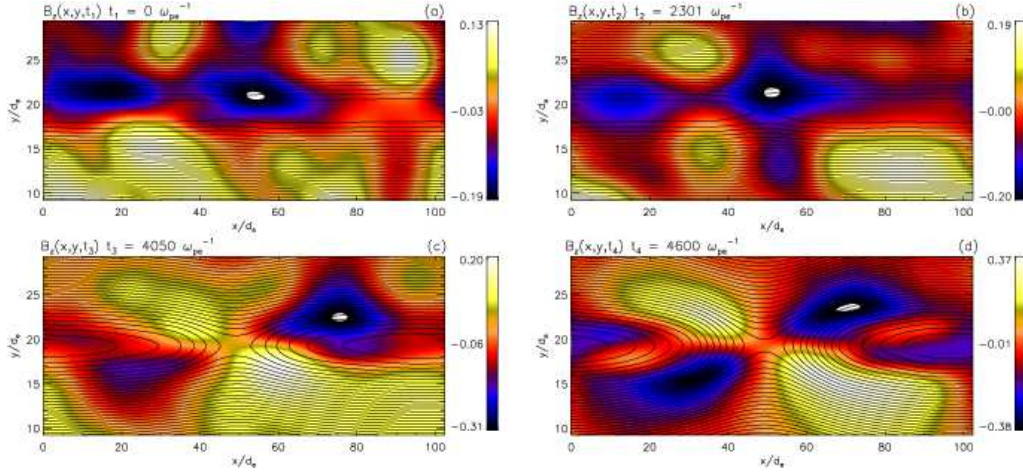


Fig. 2. Contour plots of B_z at different times. The contour lines of the magnetic flux ψ are superposed. All the panels are zoomed in y in the interval $[9 d_e, 29 d_e]$.

This code is aimed at providing significant insights into the comprehension of the electron-scale magnetic reconnection, in particular by directly comparing the low-noise results obtained through the numerical simulation with very recent *in-situ* spacecraft observations conducted by the MMS mission.

The code has been initially build up and implemented on Marconi KNL thanks to an initial INAF-B computational grant. Within the

present a INAF-A project, we have carefully tested the numerical algorithm by reproducing the dynamics of waves modes and the onset of kinetic instabilities. The development of the magnetic reconnection, for the scenario proposed in the GEM challenge (Birn 2001), has been also recovered. These results have been collected in paper, recently submitted to an international peer-reviewed journal Pezzi (2019). A preliminary performance test performed on

the Marconi-KNL cluster at CINECA super-computing center, has shown a reasonable parallel efficiency on KNL architecture Pezzi (2019). We are working to increase the code efficiency by optimizing the communication pattern of the algorithm. We are presently starting a new dedicated INAF project aimed explicitly at improving the code performance. Our main goal is to be in the conditions for applying for a PRACE project which will focus on the electron kinetic non linear dynamics in a turbulent magnetized plasma and in proximity of an X-point region around a reconnection layer.

Acknowledgements. We acknowledge the computing centre of Cineca and INAF, under the coordination of the “Accordo Quadro MoU per lo svolgimento di attività congiunta di ricerca Nuove frontiere in Astrofisica: HPC e Data Exploration di

nuova generazione”, for the availability of computing resources and support.

References

- Birn, J., et al. 2001, *J. Geophys. Res. (Space Physics)*, 106, 3715
Harris, E. G., *Nuovo Cim.* 1962, 23, 115
Mangeney, A., et al. 2002, *J. Comput. Phys.*, 179, 495
Peyret, R., Taylor, T. D. 1983, *Computational Methods for Fluid Flow* (Springer, New York)
Pezzi, O., Cozzani, G., et al., *J. of Plasma Physics*, submitted
Schmitz, H., Grauer, R. 2006, *J. Comput. Phys.*, 214, 738
Valentini, F., et al. 2007, *J. Comput. Phys.*, 225, 753